

# An Optimization Principle for Determining Movement Duration

Hirokazu Tanaka, John W. Krakauer and Ning Qian

*J Neurophysiol* 95:3875-3886, 2006. First published Mar 29, 2006; doi:10.1152/jn.00751.2005

**You might find this additional information useful...**

---

This article cites 34 articles, 8 of which you can access free at:

<http://jn.physiology.org/cgi/content/full/95/6/3875#BIBL>

Updated information and services including high-resolution figures, can be found at:

<http://jn.physiology.org/cgi/content/full/95/6/3875>

Additional material and information about *Journal of Neurophysiology* can be found at:

<http://www.the-aps.org/publications/jn>

---

This information is current as of September 6, 2006 .

# An Optimization Principle for Determining Movement Duration

Hirokazu Tanaka,<sup>1</sup> John W. Krakauer,<sup>2</sup> and Ning Qian<sup>1</sup>

<sup>1</sup>Center for Neurobiology and Behavior and Department of Physiology and Cellular Biophysics, and <sup>2</sup>Motor Performance Laboratory, Department of Neurology, Columbia University, New York, New York

Submitted 18 July 2005; accepted in final form 15 March 2006

**Tanaka, Hirokazu, John W, Krakauer, and Ning Qian.** An optimization principle for determining movement duration. *J Neurophysiol* 95: 3875–3886, 2006. First published March 29, 2006; doi:10.1152/jn.00751.2005. Movement duration is an integral component of motor control, but nearly all extant optimization models of motor planning prefix duration instead of explaining it. Here we propose a new optimization principle that predicts movement duration. The model assumes that the brain attempts to minimize movement duration under the constraint of meeting an accuracy criterion. The criterion is task and context dependent but is fixed for a given task and context. The model determines a unique duration as a trade-off between speed (time optimality) and accuracy (acceptable endpoint scatter). We analyzed the model for a linear motor plant, and obtained a closed-form equation for determining movement duration. By solving the equation numerically with specific plant parameters for the eye and arm, we found that the model can reproduce saccade duration as a function of amplitude (the main sequence), and arm-movement duration as a function of the ratio of target distance to size (Fitts's law). In addition, it explains the dependency of peak saccadic speed on amplitude and the dependency of saccadic duration on initial eye position. Furthermore, for arm movements, the model predicts a scaling relationship between peak velocity and distance and a reduction in movement duration with a moderate increase in viscosity. Finally, for a linear plant, our model predicts a neural control signal identical to that of the minimum-variance model set to the same movement duration. This control signal is a smooth function of time (except at the endpoint), in contrast to the discontinuous bang-bang control found in the time-optimal control literature. We suggest that one aspect of movement planning, as revealed by movement duration, may be to assign an endpoint accuracy criterion for a given task and context.

## INTRODUCTION

Every movement takes time. Movement duration is not arbitrary, but rather appears to depend on other parameters and on the requirements of the task and context. For example, it is known that movement duration increases with movement extent and with the endpoint accuracy requirement (Fitts 1954). Moreover, we typically do not rush to reach for a full cup of coffee or spend a whole minute to pick up a pen. These observations suggest that movement duration is not just epiphenomenal to other task variables but instead is itself a planned variable.

Despite the importance of movement duration, few extant models of motor planning are formulated to explain it. Instead, proposed models focus on the problem of trajectory redundancy: how the brain picks one stereotyped trajectory from an infinite number of possible trajectories (see, e.g., Shadmehr and Wise 2005). It is generally assumed that the brain applies

an optimization principle to single out a unique trajectory. Since the pioneering work of Flash and Hogan, several such optimization models have been proposed (Dornay et al. 1996; Flash and Hogan 1985; Harris and Wolpert 1998; Todorov and Jordan 2002; Uno et al. 1989). Although they differ greatly in the cost function being optimized (e.g., trajectory smoothness vs. endpoint accuracy), and in whether sensory feedback is used, these models all share a common feature: the movement duration is prefixed before the optimization process begins. In other words, these models assume that the movement duration is already known, and focus on determining the trajectory within this preset duration. Consequently, these models cannot predict or explain movement duration itself.

One of these models, the minimum-variance (MV) model of Harris and Wolpert (1998), has been extended to explain movement duration in Fitts's experiment. Like previous models, the MV model cannot predict movement duration. However, Harris and Wolpert (1998) introduced an additional procedure into the model to circumvent this problem: they ran the MV model multiple times with different prefixed durations and selected the duration that generated the desired endpoint accuracy. The procedure literally assumes that, before each movement, the motor system simulates many movements of different prefixed durations until a desired duration is found. Although such a trial-and-error process is plausible during motor learning, it is unlikely to be a routine component of planning simple or overlearned movements. One would have to posit a forward model that is somehow run several times before a movement is made. Alternatively, the motor system might acquire, through experience, a huge look-up table (or its function approximation) of all possible movement durations for all possible movements with all possible accuracies. Thus the biological correlates of the method used by Harris and Wolpert to generate movement duration are somewhat implausible and inefficient.

In this paper, we propose a new optimization principle that directly predicts movement duration as well as movement trajectory. Our model is closely related to the MV model, although we assign a completely different cost function. In the MV model, the variance of the endpoint position over a short postmovement period is minimized in the presence of signal-dependent neuronal noise. We also include signal-dependent noise in our model. However, we propose that it is unlikely that endpoint variance needs to be minimized absolutely but only relative to the demands of the given task. If the task is to pick up a rock, there is little reason to minimize the variance to the size of a pebble. From the perspective of survival, it may be

Address for reprint requests and other correspondence: N. Qian, Center for Neurobiology and Behavior, Columbia University, Kolb Annex Rm 519, 1051 Riverside Drive, New York, NY 10032 (E-mail: nq6@columbia.edu).

The costs of publication of this article were defrayed in part by the payment of page charges. The article must therefore be hereby marked "advertisement" in accordance with 18 U.S.C. Section 1734 solely to indicate this fact.

more useful for an animal to minimize movement duration than to minimize endpoint variance provided that the variance meets the demands of the task. For example, to escape a predator, a monkey will climb up a tree as quickly as possible, not as accurately as possible, provided that movements are accurate enough to avoid falling. For saccadic eye movements, there is another reason that time minimization may improve survival: during saccades, we are largely blind to visual inputs due to saccadic suppression (Bridgeman et al. 1975). The brain may want to minimize the impaired period of visual processing by minimizing saccade duration. There is also evidence for reduced somatosensory transmission during limb and finger movements (Ghez and Pisa 1972; Williams and Chapman 2000). Time minimization also appears appropriate for modeling the Fitts experiment in which subjects were instructed to reach any part of a target as fast as possible (Fitts 1954; Fitts and Peterson 1964). The task does not require an endpoint scatter smaller than the target size but does require minimum duration.

We therefore suggest that the brain should try to minimize movement duration under the constraint that endpoint accuracy meets a criterion demanded by the task and context, in the presence of signal-dependent neuronal noise. Here we mathematically formulate this constrained minimum-time model, analytically solve it for a linear motor plant, and demonstrate that it determines a unique movement duration. This duration reflects a trade-off between speed (time optimality) and accuracy (acceptable endpoint scatter). We then show that the model can reproduce, among other things, Fitts's law for arm movements and the main sequence for saccadic eye movements. Although we chose two well-known psychophysical results to illustrate our model, we argue that constrained time minimization is a more general principle for determining movement duration (see DISCUSSION).

Harris and Wolpert (1998) considered only minimization of endpoint variance, although they did bring up the possibility of time minimization when they wrote: "We propose that the temporal profile of the neural command is selected so as to minimize the final positional variance for a specified movement duration, or equivalently to minimize the movement duration for a specified final positional variance determined by the task." However, variance minimization and time minimization are not equivalent because cost functions of the two approaches are very different (see DISCUSSION). Hamilton and Wolpert (2002) later extended the MV model into the TOPS (task optimization in presence of signal-dependent noise) framework and applied it to obstacle avoidance; like the MV model, however, "in the TOPS framework the cost is movement error," not movement duration. In separate work, Harris (1995, 1998) did consider time minimization but without the crucial endpoint accuracy constraint. Studies of time minimization models, previously reported in the time-optimal control literature (Bryson and Ho 1975; Stengel 1986), have been proposed for both limb (Fitzhugh 1977) and eye (Enderle and Wolfe 1987; Harris 1995, 1998) movement planning. However, such models are not considered biologically plausible (see, e.g., Nelson 1983), mainly because, in the absence of an endpoint accuracy constraint, they always lead to a bang-bang control strategy where the control signal takes either the maximum or minimum value, a property contradicted by motoneuron and muscle activations, which are smooth functions

of time. Here we show that our constrained minimum-time model does not result in bang-bang control, but instead generates a smooth control signal. In fact, we will prove for the case of a linear plant that the control signal predicted by our model is identical to that of the MV model set to the same movement duration.

## METHODS

### *The constrained minimum-time model*

As argued above, we assume that the brain minimizes movement duration under the constraint that the endpoint accuracy meets a task- or context-dependent criterion and that there is signal-dependent neuronal noise in the control system. We denote the initial and final times of a movement as 0 and  $t_f$ , respectively, where  $t_f$  is the movement duration to be minimized. In our mathematical model, the endpoint accuracy constraint is actually two constraints. First, over repeated trials, the expected endpoint position of the effector should be equal to the target position during a postmovement period,  $t_p$ , which was used in the MV model (Harris and Wolpert 1998) and whose role has been analyzed mathematically by us and others (Feng et al. 2002; Tanaka et al. 2004b). Second, the mean endpoint positional variance over  $t_p$  should be bounded by a required final variance,  $V_f$ . For mathematical simplicity, we assume that the mean variance over  $t_p$  is equal to  $V_f$  in our analytical derivations. We have also simulated the case where the mean variance is less than or equal to  $V_f$  and obtain very similar results (see DISCUSSION). As with the MV model (Harris and Wolpert 1998), a nonzero  $t_p$  is needed to avoid divergence of the control signal at time  $t_f$  (Tanaka et al. 2004b). Note that, although  $V_f$  is fixed for planning a given movement, it varies according to the task and context (see *Simulation of saccades* and *Simulation of single-joint reaching*). Finally, we assume that the control signal has an additive Gaussian noise term whose SD is proportional to the control signal (signal-dependent noise) (Harris and Wolpert 1998; Todorov and Jordan 2002). The full model formulation can be found in APPENDIX A. The goal is to minimize  $t_f$  under the stated constraints and noise.

We applied the above formulation to a linear motor plant of the form

$$\theta^{(n)}(t) + \alpha_{n-1}\theta^{(n-1)}(t) + \dots + \alpha_0\theta(t) = \beta[u(t) + \xi(t)] \quad (1)$$

where  $\theta(t)$  is a scalar representing the effector position; for example, it can be the horizontal position of the eye or elbow angle.  $\theta^{(k)}(t)$  is the  $k$ th derivative of  $\theta(t)$  and Eq. 1 contains derivatives up to  $n$ th order. The coefficients  $\alpha_i$  and  $\beta$  are determined by the dynamical properties of eye and arm, and by muscle models (see *Simulation of saccades* and *Simulation of single-joint reaching*).  $u(t)$  is a scalar representing the neuronal control signal.  $\xi(t)$  is the signal-dependent noise term mentioned above, which describes trial-to-trial variability; it has a Gaussian distribution with zero mean

$$E[\xi(t)] = 0 \quad (2)$$

and a SD proportional to the control signal (Harris and Wolpert 1998). The noise is assumed to be white so that the covariance between noise at times  $t$  and  $t'$  is given by

$$E[\xi(t)\xi(t')] = Ku^2(t)\delta(t-t') \quad (3)$$

Here  $K$  is a constant that determines the noise strength and the delta function indicates that there is no correlation between noise at times  $t$  and  $t'$ . The variance of the noise at any given time is proportional to the square of the control signal at that time.

The plant in Eq. 1 has a pole-only transfer function. In general, temporal derivatives of the control signal can be added to the right-hand side of Eq. 1 to introduce zeros to the transfer function (see, e.g.,

Stengel 1986). However, we did not do so because we are not aware of any physiological evidence for such derivatives. In addition, such derivatives have the undesirable effect of amplifying signal-dependent noise. Note also that Eq. 1 contains a general motor plant that has been widely used to describe horizontal eye movements and single-joint arm movements in the literature.

For convenience, we convert Eq. 1 into a set of first-order equations in matrix form  $\dot{x} = Ax + B(u + \xi)$  by introducing an  $n$ -dimensional state vector  $x = [\theta, \dot{\theta}, \dots, \theta^{(n-1)}]^T$ . The matrices  $A$  and  $B$  are uniquely determined by the coefficients in Eq. 1 (see APPENDIX A; see also, e.g., Ogata 1998 for the state-space representation). Because we consider a point-to-point movement from a stationary initial position at  $\theta_i$  to a stationary final position  $\theta_f$ , the initial and final state vectors are given as  $x_i = (\theta_i, 0, \dots, 0)^T$  and  $x_f = (\theta_f, 0, \dots, 0)^T$ . That is, the velocity, acceleration, and higher-order temporal derivatives of the position should all be zero at the beginning and end of a movement to ensure stationarity (i.e., no systematic drift). The movement amplitude is given as a difference between the initial and final positions ( $\theta_f - \theta_i$ ). These boundary conditions are identical to those used in many previous optimization models (Flash and Hogan 1985; Harris and Wolpert 1998; Todorov and Jordan 2002; Uno et al. 1989).

With the linear plant, the constrained time-minimization problem can be solved by standard variational calculus (see APPENDIX A). Once the initial and final states ( $x_i$  and  $x_f$ ) and the final variance ( $V_f$ ) were specified, we obtained an equation that determines the movement duration  $t_f$

$$\frac{V_{f_p}}{K} = u_f^2 H(t_p) + (x_f - e^{A_f t_p} x_i)^T G^{-1}(t_p) (x_f - e^{A_f t_p} x_i) \quad (4)$$

where matrix functions  $H(t_p)$  and  $G(t_p)$  are defined in APPENDIX A.  $u_f$ , the control signal required to stabilize the plant in the desired final state for the duration of the postmovement period, equals the product of elastic constant of the motor plant and the final displacement. We call this equation (Eq. 4) the *duration equation* because  $t_f$  is the only unknown variable in this equation and it can be uniquely determined with given  $x_i$ ,  $x_f$ , and  $V_f$ . Because the duration equation is a highly nonlinear function of  $t_f$ , we resorted to numerical methods to solve for  $t_f$ .

We can also derive the optimal control signal

$$u(t) = \begin{cases} B^T e^{A^T(t-t_f)} G^{-1}(t_f) (x_f - e^{A_f t_f} x_i) / F(t) & (0 \leq t < t_f) \\ u_f & (t_f \leq t \leq t_f + t_p) \end{cases} \quad (5)$$

The definition of function  $F(t)$  is provided in APPENDIX A. This control signal is a smooth function of time except at time  $t_f$ . Thus time-optimal control does not necessarily lead to bang–bang control (Bryson and Ho 1975) when appropriate constraints are imposed. Note that this control signal solution is identical to that we derived for the MV model if the MV model is set to the same  $t_f$  (see Eqs 2.21 and 2.22 in Tanaka et al. 2004b). Therefore, for a linear plant, our model inherits the features of the MV model set to the same movement time. The main difference between the two models is that our model predicts movement time whereas the MV model does not.

### Simulation of saccades

Horizontal eye movement dynamics was modeled with a second-order differential equation

$$\ddot{\theta} + \frac{t_1 + t_2}{t_1 t_2} \dot{\theta} + \frac{1}{t_1 t_2} \theta = \tau \quad (6)$$

where  $\theta$  and  $\tau$  denote the horizontal eye displacement and the net muscle torque, respectively. We set the time constants to  $t_1 = 224$  ms and  $t_2 = 13$  ms, based on measurements in human subjects (Robinson et al. 1986). We further modeled the muscle torque  $\tau$  as a low-pass-filtered control signal  $u(t)$

$$\left(1 + t_3 \frac{d}{dt}\right) \tau = u \quad (7)$$

with the time constant  $t_3 = 10$  ms (Harris and Wolpert 1998). The two equations can be combined to give a third-order equation for the eye plant in the form of Eq. 1, with the coefficients

$$\alpha_2 = \frac{1}{t_1} + \frac{1}{t_2} + \frac{1}{t_3} \quad \alpha_1 = \frac{1}{t_1 t_2} + \frac{1}{t_2 t_3} + \frac{1}{t_3 t_1} \quad (8)$$

$$\alpha_0 = \frac{1}{t_1 t_2 t_3} \quad \beta = \frac{1}{t_3}$$

Thus the state  $x$  is a three-dimensional vector containing eye position, velocity, and acceleration.

For main-sequence simulations, we considered saccades from the primary position ( $\theta_i = 0$ ) to a stationary target located at various eccentricities [ $\theta_f$  (deg)]. The saccade amplitude was thus  $\theta_f$ . The target was assumed to have width  $W$ , which was fixed at 1.5 deg (see RESULTS for the effect of its variation). For determination of  $V_f$ , it should be noted that it cannot be assumed that the visual system foveates the target *before* the saccade; rather, for saccades of larger amplitude, the target is more eccentrically located off the fovea and thus has a lower visual resolution. This means that the visual estimation of the target becomes more variable with larger saccades and the endpoint variance of saccades must increase with saccadic amplitude even for a fixed target size. We therefore included the actually measured saccadic variability at different amplitudes in our expression of endpoint variance. Specifically, for a given target size, the SD of final eye position is a linear function of the saccade amplitude (van Opstal and van Gisbergen 1989). In addition, a larger target size means that the  $V_f$  can afford to be larger. Thus the SD of the final eye position was modeled as a sum of the target size  $W$  and a linear term of saccade amplitude  $\theta_f$ , i.e.

$$V_f = (W + a\theta_f)^2 \quad (9)$$

The slope  $a$  was fixed at 0.03, a value within the range of 0.02 to 0.05 seen in human subjects (see Fig. 5A of van Opstal and van Gisbergen 1989). We should emphasize that the dependency of variance on amplitude in Eq. 9 is a *consequence* of increased target uncertainty with amplitude. In other words, the primary factor is target uncertainty (through visual estimation) rather than amplitude per se.

We also simulated the dependency of saccadic duration on the initial eye position  $\theta_i$ . Because  $\theta_i$  took nonzero values in these simulations, saccadic amplitude was  $(\theta_f - \theta_i)$ . Equation 9 thus became

$$V_f = [W + a(\theta_f - \theta_i)]^2 \quad (10)$$

where the same values for  $a$  and  $W$  were used as in the main-sequence simulation. Note that  $V_f$  depends only on saccade amplitude ( $\theta_f - \theta_i$ ) instead of on initial positions  $\theta_i$ . This is consistent with the experimental finding that the variability of saccades is similar for different initial positions (Pelisson and Prablanc 1988).

### Simulation of single-joint reaching

We simulated single-joint movements of the forearm with the following dynamic equation (Hogan 1984)

$$I\ddot{\theta} + b\dot{\theta} = \tau \quad (11)$$

where  $\theta$  and  $\tau$  represent the elbow angle and the net muscle torque, respectively.  $I$  and  $b$  are, respectively, the moment of inertia and the intrinsic viscosity, for which we adopted the standard values of 0.25 kg · m<sup>2</sup> and 0.20 kg · m<sup>2</sup>/s for these parameters (van der Helm and Rozendaal 2000). We introduced a second-order linear muscle model with two time constants (muscle activation,  $t_a = 30$  ms, and muscle excitation,  $t_e = 40$  ms) (Winters and Stark 1985)



$$\left(1 + t_a \frac{d}{dt}\right) \left(1 + t_e \frac{d}{dt}\right) \tau = u \quad (12)$$

and obtained the fourth-order plant for the forearm with coefficients

$$\alpha_3 = \frac{b}{I} + \left(\frac{1}{t_a} + \frac{1}{t_e}\right) \alpha_2 = \frac{1}{t_a t_e} + \left(\frac{1}{t_a} + \frac{1}{t_e}\right) \frac{b}{I} \quad (13)$$

$$\alpha_1 = \frac{b}{t_a t_e I} \quad \alpha_0 = 0 \quad \beta = \frac{1}{t_a t_e I}$$

The four-dimensional state vector contains hand position, velocity, acceleration, and jerk.

We simulated different movement distances ( $D$ ) and target widths ( $W$ ). Movement distance was a product of the forearm length ( $L_0$ ) and an elbow-angle amplitude ( $\theta_f - \theta_i$ ), i.e.,  $D = L_0(\theta_f - \theta_i)$ . The forearm length was set to 0.35 m (Uno et al. 1989). We required that any part of a finger tip of width  $w$  overlap the target with a 95% probability of success (Harris and Wolpert 1998). Accordingly, we set

$$V_f = (W + w)^2 / r^2 \quad (14)$$

with  $r = 1.96$  to ensure a 95% success rate because the final position is approximately Gaussian in distribution. The finger size  $w$  was fixed at 0.6 cm (Harris and Wolpert 1998). The assumption is that the visual system is able to provide accurate measures of  $w$  and  $W$  by foveating on the finger and target before the reaching movement. Thus unlike the saccadic variance Eq. 9, there is no amplitude dependency in Eq. 14. The sum of the widths in Eq. 14 determines the allowed variability for the finger to hit the target.

### Numerical methods

All the simulations were performed with Matlab (The MathWorks, Natick, MA) on a Linux computer. For numerical solutions of the duration Eq. 4, we used Simpson's method to evaluate the integral in the matrix  $G$  and applied the bisection method to find the optimal movement duration (see, e.g., Press et al. 1992). The model has two main free parameters: the noise intensity  $K$  and the postmovement duration  $t_p$ . We adjusted these parameters to fit the experimental data. We also confirmed that the model depends smoothly on the choice of the parameter values. In particular, we found that the results do not change significantly for  $t_p > 50$  ms for eye movements and  $> 200$  ms for arm movements.

## RESULTS

Our main analytical results for a linear plant, derived in the APPENDIX A, are that the constrained time-minimization model can determine a unique movement time according to Eq. 4 (the duration equation), and that the control signal Eq. 5, and thus the movement trajectory determined by our model, are identical to those given by the MV model set to the same movement duration. In this section, we present results from our numerical solutions of the duration equation and show that the main

sequence of saccadic eye movements, the dependency of duration on initial eye position, and Fitts's law of arm movements can all be explained by this equation.

### The saccadic main sequence

Figure 1A shows that our model reproduces the main sequence: the linear relationship between saccadic amplitude and duration (Bahill et al. 1975; Baloh et al. 1975). In this set of simulations, we set the postmovement duration to  $t_p = 100$  ms and the noise proportionality constant to  $K = 5.5 \times 10^{-4}$ . The movement durations were calculated with saccadic amplitudes ranging from 2.5 to 50 deg. For comparison, we reproduced in Fig. 1B the corresponding experimental data taken from van der Geest and Frens (2002). There is close agreement between the simulation and the data. In addition to the linear relation at relatively larger saccade amplitudes, the model can also explain the downturn at smaller amplitudes. Although we used a particular set of parameter values in Fig. 1A to match the data in Fig. 1B, we observed similar linear relationships with many other parameter combinations; the difference was mainly in the slopes and intercepts of the line. In particular, we always obtained a nearly linear relationship with target sizes  $W > 1.0$  deg. When the target size was  $< 1.0$  deg, the duration–amplitude plot became somewhat curved but remained a monotonically increasing function, consistent with the experimental data.

After determining the optimal duration, we calculated the optimal control signal predicted by our model according to Eq. 5, and the corresponding movement trajectory. The model predicts that the peak velocity is a monotonically increasing function of the amplitude with a gradual fall-off in slope (Fig. 2A), again in close agreement with experimental data (Baloh et al. 1975; van der Geest and Frens 2002). Note that previous optimization models, including the MV model, cannot predict peak velocity values without extra assumptions because peak velocity critically depends on duration. The velocity profiles and the optimal control signals obtained with our model (results not shown) are identical to those of the MV model (Harris and Wolpert 1998) set to the same movement times, as we have already shown analytically (see METHODS).

Harris (1998) demonstrated that bang–bang control derived through time minimization can explain the main sequence but not the shape of the velocity profile. In contrast, our constrained time-minimization model avoids nonphysiological bang–bang control and explains both the main sequence and the shape of velocity profiles.

Saccadic duration is known to be dependent not only on amplitude but also on initial eye position. In particular, several

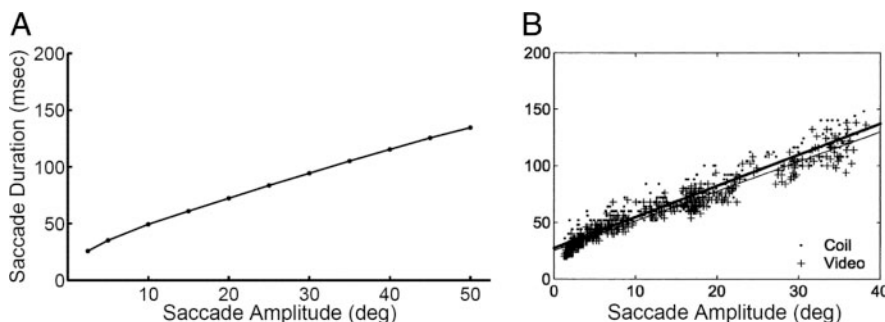


FIG. 1. Main sequence for saccadic eye movements (the linear relationship between saccadic duration and amplitude). *A*: model simulation. *B*: corresponding experimental data taken from van der Geest and Frens (2002), with permission from Elsevier. Data were obtained with both the scleral search coil method (dots) and a video-based 2D eye-tracking method (crosses).

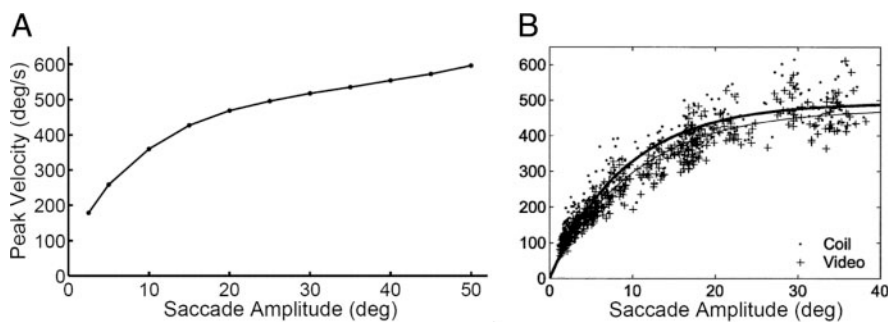


FIG. 2. Peak velocity as a function of saccadic amplitude. *A*: model simulation. *B*: corresponding experimental data taken from van der Geest and Frens (2002), with permission from Elsevier. Data were obtained with both the scleral search coil method (dots) and a video-based 2D eye-tracking method (crosses).

studies found that centrifugal saccades (i.e., away from the primary position) are slower than centripetal saccades (i.e., toward the primary position) of the same amplitude (Abel et al. 1979; Eggert et al. 1999; Pelisson and Prablanc 1988). Figure 3*C* shows experimental data taken from Pelisson and Prablanc (1988). A subject made 30-deg saccades from three different starting positions  $\theta_i$ : 1)  $\theta_i = 0$  and  $\theta_f = 30$  deg. The saccade was purely centrifugal, from the primary position to a point of 30-deg eccentricity (the curve marked with filled circles). 2)  $\theta_i = -10$  deg and  $\theta_f = 20$  deg. The saccade was 10-deg centripetal and 20-deg centrifugal, from a point of 10-deg eccentricity, through the primary position, and to a point of 20-deg eccentricity on the other side (the curve marked with filled triangles). 3)  $\theta_i = -20$  deg and  $\theta_f = 10$  deg. The saccade was 20-deg centripetal and 10-deg centrifugal, from a point of 20-deg eccentricity, through the primary position, and to a point of 10-deg eccentricity on the other side (the curve marked with filled squares). We simulated these three saccades with the same parameters as used in the main-sequence simulations above and the results are shown in Fig. 3*A*. There is good

qualitative agreement between the simulations and the data, with the purely centrifugal saccade taking a longer time than that with a centripetal component. We also found that a 55% increase of the  $K$  parameter can produce a more quantitative agreement between the model's prediction (Fig. 3*B*) and the data (Fig. 3*C*). Adjusting the parameter  $K$  is justified because there is considerable intersubject variability in the magnitude of signal-dependent noise (Jones et al. 2002), and the main-sequence data (Figs. 1*B* and 2*B*) and the data here (Fig. 3*C*) are taken from different experiments with different subjects.

It is important to note that because the saccadic amplitude ( $\theta_f - \theta_i$ ) was fixed at 30 deg, the endpoint variance (Eq. 10) used in our simulations did not depend on initial eye position  $\theta_i$ . This is consistent with the experimental finding that saccade variability was similar for the three different initial eye positions (Pelisson and Prablanc 1988). The reason that the simulated saccadic duration depends on initial eye position is the presence of an elastic restoration force in the eye plant (the third term of Eq. 6). Because this force results from elastic connective tissues instead of from neuronal control signal, it is

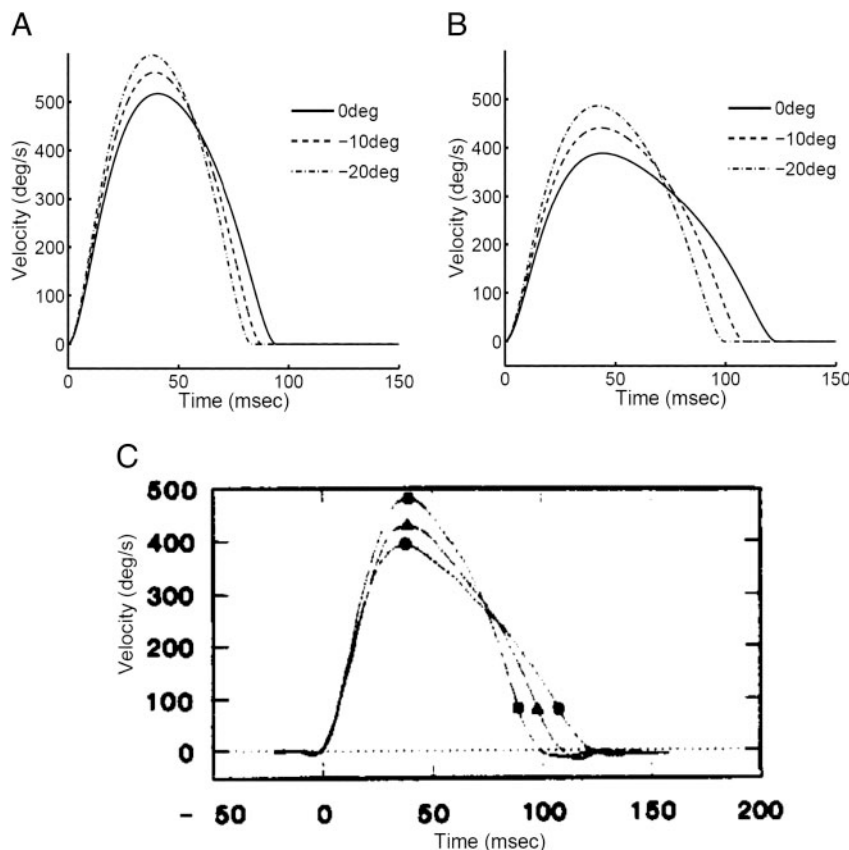


FIG. 3. Dependency of saccadic duration on initial eye position. Saccadic amplitude was fixed at 30 deg. Initial eye position was 0, -10, and -20 deg from the primary position for the 3 curves in each panel. *A*: simulations with the same set of parameters as in Figs. 1 and 2. *B*: simulations with a 55% increase in  $K$  value without changing other parameters. *C*: corresponding experimental data, taken from Pelisson and Prablanc (1988) with permission from Elsevier. Curves marked with filled circles, triangles, and squares are for initial positions that were 0, -10, and -20 deg away from the primary position, respectively.

not accompanied by signal-dependent noise. Centripetal saccades are facilitated by this noise-free elastic force. In contrast, centrifugal saccades have to overcome the elastic force. A larger control signal cannot fully cancel the effect of the elastic force because the increased signal-dependent noise will generate a greater endpoint variation. A longer duration is thus needed to ensure accuracy of the saccade. Our explanation provides a simpler and more quantitative (but not mutually exclusive) alternative to that offered by Pelisson and Prablanc (1988). They suggested that saturation in oculomotor neuron activity and/or nonlinear length-tension relationship in extraocular muscles could cause the kinematic differences in centrifugal and centripetal saccades, but did not provide quantitative evidence.

#### Fitts's law

Fitts's law quantifies the intuitively unsurprising notion that it takes a longer time to reach for a smaller or more distant target. It is expressed as  $t_f = a_1 + a_2 \log_2(2D/W)$  (see a reproduced plot in Fig. 4C), where  $W$  is the target size,  $D$  is the movement distance, and  $a_1$  and  $a_2$  are empirical constants (Fitts 1954). An important feature of Fitts's law is that movement

duration depends only on the ratio of movement distance to target size, instead of on each parameter separately.

Our model reproduces Fitts's law. First, by examining the duration Eq. 4, we can show analytically that duration is determined by the ratio of  $D$  and  $W$  when the finger size ( $w$ ) is negligible. Specifically, we prove that with the linear arm model of Eq. 11, the duration Eq. 4 can be reduced to a much simpler form (see APPENDIX B)

$$C \cdot \left(\frac{W+w}{D}\right)^2 = g(t_f) \quad (15)$$

where  $C = t_p L_0^2 / r^2 K$ ,  $L_0$  is the forearm length, and  $g(t_f)$  denotes the (1,1)-component of the matrix  $G^{-1}(t_f)$ . Equation 15 clearly indicates that the duration  $t_f$  is a function of  $D/(W+w)$ . When the finger width is negligibly small compared with the target size, the duration is dependent only on the ratio  $D/W$ , as in Fitts's law.

Second, with Eq. 4 (or equivalently with Eq. 15), we simulated the predicted movement duration numerically. Figure 4, A and B shows the results plotted against the index of difficulty (ID),  $\log_2(2D/W)$ . For these simulations, we chose a postmovement duration  $t_p = 400$  ms, and the noise proportionality constant  $K = 5 \times 10^{-5}$ . We also confirmed that the qualitative features of the results remained invariant under

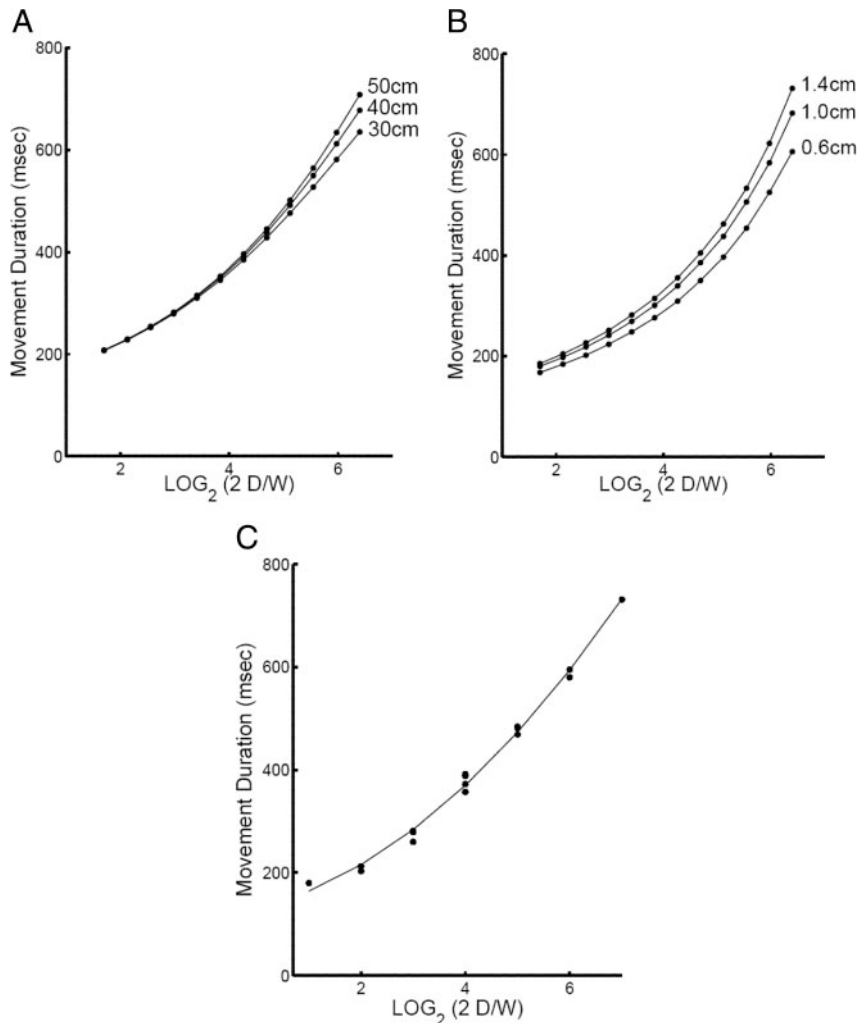


FIG. 4. Arm movement duration as a function of index of difficulty  $\log_2(2D/W)$ . A and B: model simulations. A:  $W$  was varied for 3 fixed  $D$  values (30, 40, 50 cm). B:  $D$  was varied for 3 fixed  $W$  values (0.6, 1.0, 1.4 cm). C: experimental data replotted from Fitts (1954).

many other parameter combinations. The three curves in Fig. 4A were for reaching movements with fixed distances of 30, 40, and 50 cm, respectively. Each curve was obtained by varying the target width. When the ID is small (i.e., the target width is large) the three curves overlap and the duration depends only on the ID as predicted by our analytical result above. Each curve becomes roughly linear at large values of ID, in accordance with the logarithmic form of Fitts's law. For comparison, we replotted Fitts's data in Fig. 4C. The three curves in Fig. 4B were for reaching movements to targets of fixed width of 0.6, 1.0, and 1.4 cm, respectively. Each curve was obtained by varying the movement distance. Although the curves are somewhat more curved than those in Fig. 4A, the qualitative features of the curves are similar to the logarithmic Fitts's law. Interestingly, we found that the curves in Fig. 4B can be well fit by a power law of the form:  $t_f = a_1(D/W)^{a_2}$ . Previous experimental studies have noted deviations from the log form of Fitts's law (Schmidt and Lee 1998). The power law has been suggested as a more accurate alternative for fitting duration data (Schmidt and Lee 1998). Indeed, even for simulations in Fig. 4A and Fitts's original data replotted in Fig. 4C, the power law provides a better fit than the log law. The residual errors are 0.0050 and 0.012 for the power-law and log-law fits of Fitts's data, respectively. A problem with the log law is its divergence at small  $D$ . The power law avoids this problem.

We also predicted how peak velocity ( $p_v$ ) scales with the movement distance ( $D$ ) (Fig. 5). The three curves in the figure were obtained with the target size  $W$  fixed at 0.6, 1.0, and 1.4 cm, respectively. These curves are roughly linear with the same slope in the log-log plot, indicating a power-law relationship  $p_v = (\text{const.}) \times D^\delta$ . Curve fitting of these and additional simulation results (not shown) confirmed that the value of the exponent remains in a relatively narrow range of [0.50, 0.55] when the target size is varied from 0.3 to 3.0 cm.

Finally, we explored how movement duration depends on the dynamic parameters of the plant. We found that the effect of viscosity is particularly interesting because our model makes an initially unexpected prediction: movement duration should decrease with increasing viscosity (Fig. 6). In these simulations, we assumed that in addition to the intrinsic viscosity  $b$  in

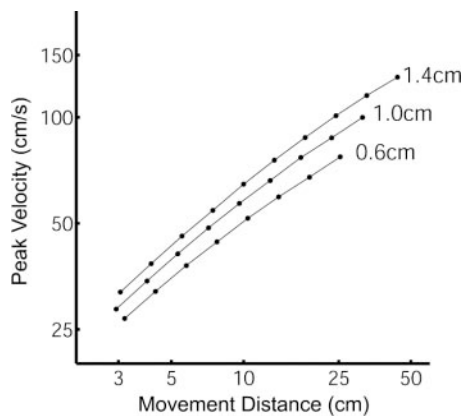


FIG. 5. Simulation of arm movement peak velocity as a function of movement distance. Three curves were obtained by fixing target size at 0.6, 1.0, and 1.4 cm, respectively. Note that a logarithmic scale is used for both axes.

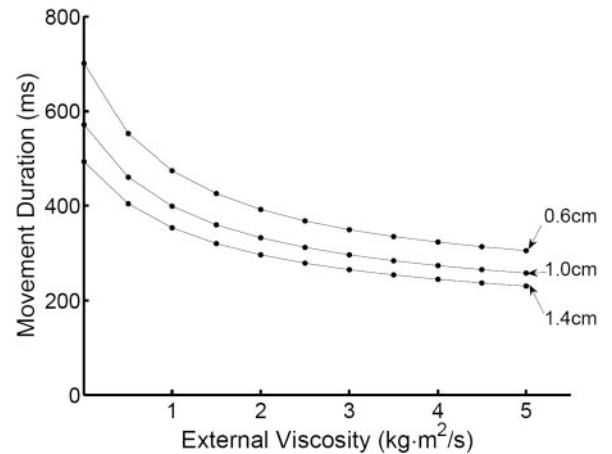


FIG. 6. Simulation of movement duration as a function of external viscosity. Movement distance was fixed at 25 cm and 3 target sizes (0.6, 1.0, and 1.4 cm) were considered.

Eq. 11, there is an externally imposed viscosity  $\tilde{b}$  so that Eq. 11 was replaced by

$$I\ddot{\theta} + (b + \tilde{b})\dot{\theta} = \tau \tag{16}$$

where  $\tilde{b}$  ranged from 0 to  $5 \text{ kg}\cdot\text{m}^2/\text{s}$  in increments of 0.5. Three different target sizes (0.6, 1.0, and 1.4 cm) were simulated for a movement distance of 25 cm (similar results were obtained for other parameter combinations). This prediction may at first appear counterintuitive because it asserts that a higher resistive viscous force makes the movement go faster. However, it actually makes good sense: improved system stability at higher viscosity reduces the propagation of signal-dependent noise through time (Tanaka et al. 2004b) and the system can thus afford to use a larger control signal without violating the endpoint accuracy constraint. This is analogous to the case of walking on ice. To avoid falling, we have to walk more slowly than the maximum speed we could achieve on ice. However, if the ice is sprinkled with sand, resistance increases, stability improves, and we can afford to walk a little faster.

In the limiting case of extremely high viscosity, the movement must be slower because it becomes very difficult to move. Our model fails to predict an increase of duration in this limit because we did not include a control cost (a measure of energy consumption) in the cost function and so the control signal can grow without bound. With this limitation in mind, we predict that with increasing viscosity, the movement should first become faster and then slow down.

DISCUSSION

In this paper, we propose a novel optimization principle that—unlike previous models that determine trajectory only—can also determine movement duration. Our main hypothesis is that it is evolutionarily adaptive to move as fast as possible for the degree of accuracy that is selected for the given task and context. Specifically, we assume that the brain minimizes movement duration in the presence of signal-dependent noise and under the constraint of an acceptable endpoint scatter around the target position. We solved this constrained minimum-time model analytically for linear motor plants and obtained a closed-form equation for determining the movement duration (the duration equation Eq. 4). Our analysis also



proved that for linear plants, the control signal (and thus muscle torque and movement trajectory) predicted by our model is identical to that predicted by the MV model set to the same movement time. However, there is no general equivalence between our model and the MV model because they use very different cost functions (see following text). Because the predicted control signal is a smooth function of time, our work demonstrates that time-optimal control does not necessarily lead to discrete bang–bang control when appropriate constraints are applied. For arm movements, the duration equation can be transformed to analytically prove part of Fitts's law: that movement duration depends only on the ratio of movement distance to target width, instead of on each parameter separately. The full Fitts's law relationship and its power-law variant are obtained through numerical solutions of the duration equation. Numerical simulations also predict the saccadic main sequence—the relationship between saccadic duration and amplitude—and the dependency of saccadic duration on initial eye position. Furthermore, our work provides a new explanation of why centrifugal saccades are slower than centripetal ones of the same amplitude. A centrifugal saccade has to overcome the restoration force of the elastic tissue. A larger control signal cannot fully cancel the effect of the elastic force because the increased signal-dependent noise would generate greater endpoint variance.

We should emphasize that we used standard eye and arm models and parameters in our simulations. As mentioned in METHODS, the only free parameters adjusted to fit the experimental data are the postmovement duration  $t_p$  and the noise proportionality constant  $K$ . Because the results are not sensitive to  $t_p$  for large values of  $t_p$  ( $\geq 50$  ms for eye and  $\geq 200$  ms for arm movements),  $K$  is the main free parameter of the model. Note that at the level of abstraction used in our model,  $K$  is not the noise strength of a single neuron, which would be more or less fixed. Rather,  $K$  measures the noise strength of the neuronal population that generates the control signal. Decreasing  $K$  is thus equivalent to increasing the number of cells in the population. It is this interpretation of  $K$  that justifies its use as a free parameter.

Despite its simplicity, our model makes several testable predictions. First, for the main-sequence simulation in Fig. 1A, the linear relationship between the duration and amplitude depends on a constant saccadic target size. The model predicts that the linear relationship should be violated if, for example, the target size scales with the amplitude. Second, the small divergence of the three curves in Fig. 4A is caused by a nonzero finger width used in the simulations. The model predicts greater divergence for single-joint movements if the finger width is increased artificially, say, by wearing a glove. Third, Fig. 5 shows the model's prediction of the relationship between peak velocity and movement distance for single-joint movement. Finally, the model predicts a reduced movement duration with a moderate increase of viscosity (Fig. 6).

The endpoint accuracy constraint used in our analyses and simulations required the variance averaged over a postmovement duration to *equal* a criterion. However, one may argue that it would be more reasonable to require that the variance be *less than* or *equal to* the criterion. We also ran a simulation with this inequality constraint and the results (not shown) are very similar to those with the equality constraint. This is because to minimize movement duration, the largest allowed

control signal, and thus the largest allowed noise in the control signal, should be used. The characteristics of the plant, which determine how noise propagates through time (Tanaka et al. 2004), are such that the largest allowed variance will be realized at the end of a movement. Consequently, the inequality constraint reduces to the equality constraint for our simulations. An exception occurs when movement extent approaches zero. Under this condition, the control signal and thus signal-dependent noise approach zero and there is no movement variability to satisfy the equality constraint. Thus the inequality constraint has to be used in this special case and the predicted movement duration is zero because it is the shortest time that satisfies the inequality constraint.

In our model, the speed–accuracy trade-off is described as the minimum duration needed to achieve a predetermined endpoint scatter. In the MV model, the trade-off is described as the minimum variance achievable within a predetermined duration. Intuitively, one might argue that there is an obvious equivalence between the two models. The argument would go that the MV model fixes the duration and finds the variance, whereas our model fixes the variance and finds the duration, and thus the two models must be equivalent. However, such intuition is logically flawed. A hidden assumption in such an argument is that there is a fixed, one-to-one relationship between endpoint variance and movement duration. However, the variance–duration relationship is not a starting premise but the solution of an optimization process and thus depends on the choice of cost function. The MV model and our model use completely different cost functions. Consequently, there is no a priori reason to believe that they will generate the same variance–duration relationship. Therefore one should not assume equivalence between the two models without a rigorous mathematical demonstration. Indeed, to the best of our knowledge, ours is the first such demonstration for linear plants. For nonlinear plants, the two models are likely to be different; or at the very least, equivalence would need to be rigorously demonstrated.

Even for a linear plant, where there is indeed mathematical equivalence between our model and the MV model, there is still an important distinction between the models in terms of biological plausibility. Consider the case of reaching out to touch a target of a certain size (such as pushing a button). Our model says that vision provides an estimate of target size and location, which can be used to determine the movement duration and control signal so that we successfully hit the target in one trial. In contrast, the MV model requires movement duration to be fixed at an arbitrary value. If we miss the target or touch it with unnecessary precision, we then adjust the preset movement duration accordingly. The process is then repeated iteratively until an optimal duration is found. This is literally what Harris and Wolpert (1998) did in their simulation of Fitts's law. If the time spent on trial and error is taken into account, the movement is no longer the fastest allowed. Alternatively, the MV model could assume that the brain stores a huge look-up table (or its function approximation) containing the movement durations for all possible movements at all possible accuracies that one is ever going to encounter. This assumption simply converts the original problem into a new one, i.e., how this huge table or its approximation is acquired and stored and how it should be structured to allow quick retrieval of an entry. In our model, sensory inputs provide a

natural basis for choosing the required endpoint accuracy, which then starts the optimization process. In contrast, in the MV model, there is no obvious biological basis for picking the right movement duration before the optimization process starts.

The above discussion also suggests that it should be easier to implement our model than the MV model in neural or artificial systems. In particular, even after a neural circuit has already learned the optimization procedure, the MV model still has to rely on trial and error or to acquire a huge look-up table to determine the movement duration. In contrast, our model can simply feed the sensory estimate of target size and location into the optimization circuit.

It should also be pointed out that Wolpert and colleagues only numerically solved their MV model. In contrast, we solved our constrained minimum-time model analytically and compared it with our previous analytical solution of the MV model (Tanaka et al. 2004b).

Although our constrained time-minimization model appears particularly appropriate for understanding fast eye and arm movements, the model may be applicable to movement planning in general. According to our model, the brain favors the fastest movement that can satisfy the desired endpoint accuracy. Thus slow movements do not necessarily contradict our model; in our framework, the movement is slow because the subject has set a very stringent accuracy criterion for the task. Likewise, if a subject performs the same motor task with different durations under different contexts, our interpretation would be that the different contexts demand different endpoint accuracies. Indeed, a tennis player's second serve is usually slower than the first serve because higher accuracy is demanded to avoid a double fault. Therefore to understand movement planning, it is critical to know the desired accuracy set by the subject. In the Fitts paradigm, accuracy is explicitly determined by the instruction to land anywhere within the target. In many other motor control experiments and for natural movements made outside the laboratory, an accuracy requirement is not explicitly imposed but instead is set implicitly by the subject depending on object size, task, and context. We suggest that to understand movement duration it is necessary to measure the actual endpoint variance over repeated trials to reveal the implicit accuracy criterion.

The above discussion leads to a more general interpretation of the simulation results in Figs. 4 and 5 for the Fitts experiment. Take Fig. 5 as an example. This figure shows the predicted peak velocity as a function of movement distance at three different target sizes for the Fitts paradigm. However, if the brain generally prefers the fastest movement that satisfies an endpoint accuracy criterion, then the predictions should be applicable to different non-Fitts contexts. The only difference is that under the Fitts paradigm, subjects are explicitly told to use the target size as the endpoint accuracy criterion, whereas in other contexts, subjects choose an implicit criterion that needs to be revealed by measuring the endpoint scatter over repeated trials. Therefore if we interpret the three target sizes in Fig. 5 as three different internal criteria, then the predictions in the figure should be valid in general: that is, if the same subject makes the same movement trajectory to the same target in three different contexts and happens to show three different levels of endpoint accuracy as in Fig. 5, then the three curves in the figure are the predicted velocity–distance relationships.

Like many previous optimization models (Dornay et al. 1996; Flash and Hogan 1985; Harris and Wolpert 1998; Uno et al. 1989), our constrained minimum-time model is purely feedforward, and does not take sensory feedback signal into account. Feedforward planning may be appropriate for well-practiced movements, but sensory feedback can have a profound influence on the motor planning and trajectory formation (Carlton 1981; Keele and Posner 1968; Sober and Sabes 2005; Tanaka et al. 2004a; Todorov and Jordan 2002). Indeed, a qualitative account of Fitts's law based on sensory feedback and corrective submovements has been suggested (Crossman and Goodeve 1983; Keele 1968). In future work we plan to extend our constrained minimum-time model by including sensory feedback in a manner proposed by Todorov and Jordan (2002) and then compare feedforward- and feedback-based accounts of Fitts's law.

Another potentially useful extension of our model would be an inclusion of a control cost term in the cost function. Control cost measures the energy consumption of a movement. It seems reasonable to assume that when a movement is relatively easy and brief, as is the case for the Fitts experiment and saccadic eye movements, factors such as energy consumption and muscle fatigue are not important. On the other hand, for difficult movements (such as weight lifting, extremely high viscosity) or repetitive movements (such as running), these factors are likely to be relevant. In such cases, the variability in duration of the same movement trajectory may be explained by the variation in the relative weighting between time minimization and energy minimization, in addition to variation in task- and context-dependent accuracy criteria.

APPENDIX A: DETAILED FORMULATION OF THE MODEL AND ITS SOLUTION

Here we describe the model formulation, and derive the duration Eq. 4 and the optimal control signal Eq. 5. As we explained in the text, we assume that the brain minimizes movement duration  $t_f$  under the constraint that the endpoint accuracy of the movement meets the criterion for the current task. To describe the model concisely, we use both the scalar  $[\theta(t)]$  and vector  $[x(t)]$  notations, where  $\theta$  is the effector position and  $x = [\theta, \dot{\theta}, \dots, \theta^{(\alpha-1)}]^T$  is the state vector. The accuracy constraint can be expressed as two equality constraints. The first is the final position constraint, which requires that at each moment in the postmovement duration ( $t_p, t_f + t_p$ ), the expected effector position  $\theta$  equals the desired target location  $\theta_f$ , and that temporal derivatives of  $\theta$  equal 0 (to avoid drift after the movement). In vector notion, we have

$$x_f = E[x(t)] \quad (t_f \leq t \leq t_f + t_p) \tag{A1}$$

where  $x_f = (\theta_f, 0, \dots, 0)^T$ . The second constraint is the final variance constraint, which requires that the effector variance averaged over the postmovement duration equals a fixed, task-dependent value  $V_f$

$$V_f = \frac{1}{t_p} \int_{t_f}^{t_f+t_p} dt \text{Var} [\theta(t)] \tag{A2}$$

Here we focused on the variance of  $\theta(t)$  instead of using the full covariance matrix of  $x(t)$  because the former provides the most direct measure of the movement accuracy. The relationship between the other elements of the covariance matrix and the movement accuracy is not straightforward. In addition, there are considerably fewer data available on the other elements of the covariance matrix such as the variance of acceleration or the covariance between velocity and jerk.

Thus there is little information on how to set constraints on those elements.

The optimization process with the equality constrains can be solved with the Lagrange multiplier method. The augmented cost function is

$$S_{MT}[t_f, u(t); \lambda, \mu(t)] = t_f + \lambda \left[ V_f - \frac{1}{t_p} \int_{t_f}^{t_f+t_p} dt \text{Var} [\theta(t)] \right] + \int_{t_f}^{t_f+t_p} dt \mu^T(t) \{x_f - E[x(t)]\} \quad (A3)$$

where  $\lambda$  and  $\mu(t)$  are Lagrange multipliers.  $t_f$  and  $u(t)$  over  $0 \leq t \leq t_f + t_p$  are varied to minimize  $S_{MT}$ .

Although the above constrained minimum-time model could be applied to any motor plant, we restrict ourselves to a linear dynamics Eq. 1 to obtain a closed analytical solution. With the state-space representation  $x = (\theta, \dot{\theta}, \ddot{\theta}, \dots)^T$ , the  $n$ th order differential Eq. 1 is reduced to a set of first-order equations in matrix form

$$\dot{x} = Ax + B(u + \xi) \quad (A4)$$

where the dynamical matrices are

$$A = \begin{bmatrix} 0 & 1 & 0 & \dots & 0 \\ 0 & 0 & 1 & \dots & 0 \\ 0 & 0 & 0 & \dots & 0 \\ \vdots & \vdots & \vdots & \ddots & \vdots \\ -\alpha_0 & -\alpha_1 & -\alpha_2 & \dots & -\alpha_{n-1} \end{bmatrix} \quad B = \begin{bmatrix} 0 \\ 0 \\ \vdots \\ 0 \\ \beta \end{bmatrix} \quad (A5)$$

The components for the eye and arm matrices are already given in METHODS. Equation A4 has the following formal solution

$$x(t) = e^{At}x_i + \int_0^t dt' e^{A(t-t')}B[u(t') + \xi(t')] \quad (A6)$$

Using the noise model in Eq. 2, we can then explicitly evaluate the right-hand side of the final position constraint (Eq. A1) as a linear functional of the control signal

$$x_f = E[x(t)] = e^{At}x_i + \int_0^t dt' e^{A(t-t')}Bu(t') \quad (t_f \leq t \leq t_f + t_p) \quad (A7)$$

Similarly, the formal solution (Eq. A6) and the noise model (Eqs. 2 and 3) can be used to derive the expected full covariance matrix of  $x(t)$  as  $K \int_0^t dt' e^{A(t-t')}BB^T e^{A'(t-t')}$ . By extracting the (1,1)-component of the covariance matrix, we can express the right-hand side of the final variance constraint (Eq. A2) as a quadratic functional of the control signal

$$V_f = \frac{1}{t_p} \int_{t_f}^{t_f+t_p} dt \text{Var} [\theta(t)] = \frac{K}{t_p} \int_{t_f}^{t_f+t_p} dt \int_0^t dt' f(t'; t)u^2(t') \quad (A8)$$

Here  $f(t'; t)$  is the (1,1)-component of the matrix  $e^{A(t-t')}BB^T e^{A'(t-t')}$ . This function  $f(t'; t)$  is the weighting factor describing how much signal-dependent noise at time  $t'$  contributes to the positional variance at a later time  $t$  (Tanaka et al. 2004b).

We used a shortcut to simplify the above variational problem. Because the target is always at position  $\theta_p$  after  $t_f$  the control signal should balance the elastic force of the plant ( $u_f = \alpha_0\theta_f/\beta$ ) to maintain the plant at the target location after the movement. By fixing the postmovement control signal to  $u_f$ , the positional constraint Eq. A1 is automatically satisfied after the movement ( $t_f < t \leq t_f + t_p$ ), and we only need to enforce the positional constraint at time  $t_f$ :  $x_f = E[x(t_f)]$ . With the fixed control signal in the postmovement duration, the final variance constraint (Eq. A8) can also be simplified to

$$\frac{V_f}{K} = \int_0^{t_f} dt F(t)u^2(t) + u_f^2 H(t_p) \quad (A9)$$

where the functions  $F(t)$  and  $H(t_p)$  are defined as integrals of the weighting factor

$$F(t) = \int_{t_f}^{t_f+t_p} dt' f(t'; t) \quad (A10)$$

and

$$H(t_p) = \int_{t_f}^{t_f+t_p} dt \int_{t_f}^t dt' f(t'; t) \quad (A11)$$

The first and second terms in the right-hand side of Eq. A9 represent the contribution of noise during and after the movement, respectively. Equation A3 can then be reduced to a simpler cost function

$$\tilde{S}_{MT}[t_f, u(t); \lambda, \mu] = t_f + \lambda \left[ V_f - \frac{1}{t_p} \int_{t_f}^{t_f+t_p} dt \text{Var} [\theta(t)] \right] + \mu^T [x_f - E[x(t_f)]] \quad (A12)$$

By substituting the explicit forms of Eqs. A7 and A9 for the constraints, and applying the calculus of variation to Eq. A12 with respect to  $t_f$  and  $u(t)$  ( $0 \leq t < t_f$ ), we obtain the necessary conditions for time optimality

$$0 = \frac{\partial \tilde{S}_{MT}}{\partial t_f} = 1 - \frac{\lambda}{t_p} \left[ \int_0^{t_f+t_p} dt f(t; t_f + t_p)u^2(t) - \int_0^{t_f} dt f(t; t_f)u^2(t) \right] \quad (A13)$$

$$0 = \frac{\delta \tilde{S}_{MT}}{\delta u(t)} = 2K\lambda F(t)u(t) + \mu^T e^{-At}B \quad (A14)$$

In deriving Eq. A13, we used  $\partial E[x(t_f)]/\partial t_f = 0$  based on Eq. A7, so there is no  $\mu$ -dependent term. Equation A14 gives

$$u(t) = -\frac{\mu^T e^{-At}B}{2K\lambda F(t)} \quad (A15)$$

Substituting this control signal expression into the final position constraint Eq. A7 we obtain the ratio of the multipliers

$$\frac{\mu}{\lambda} = 2KG^{-1}(t_f)(x_i - e^{-At_f}x_f) \quad (A16)$$

where matrix  $G$  is defined as

$$G(t_f) \equiv \int_0^{t_f} dt \frac{e^{A(t_f-t)}BB^T e^{A'(t_f-t)}}{F(t)} \quad (A17)$$

analogous to the Grammian matrix for a linear, time-invariant system (Bryson and Ho 1975; Stengel 1986). The matrix  $G$  has to be nonsingular for the ratio of the multipliers to exist, analogous to the nonsingular requirement on the Grammian matrix for achieving controllability [4, 32]. For the eye and arm plants used in the simulations,  $G$  values are indeed invertible. Substituting this ratio of multipliers into Eq. A15, we obtain the optimal control signal (Eq. 5). Note that the optimal control signal does not explicitly depend on the noise proportionality constant  $K$ . The duration Eq. 4 is obtained by substituting the optimal control signal expression into the final variance constraint (Eq. A9). Finally, the multipliers are determined by Eqs. A13 and A16.

Note that the time optimization condition (Eq. A13) is not explicitly used to derive the optimal control signal and the duration equation, but only to determine the Lagrange multipliers. This is a common feature



of all time-optimal control problems with a linear constraint of  $u(t)$  and a quadratic constraint of  $u(t)$  (Smith 1974). Because of this feature, the same optimal control signal and movement duration can be obtained when the cost function  $t_f$  is replaced by any monotonically increasing function of  $t_f$ .

APPENDIX B: DERIVATION OF EQ. 15

Here, by partially evaluating the matrix exponential  $e^{At_f}$ , we derive the simpler form (Eq. 15) of the duration Eq. 4 when there is no elastic force in the dynamics of the linear plant, which is the case for single-joint reaching. As explained in METHODS, by combining the two second-order differential equations (Eqs. 11 and 12) for single-joint dynamics and muscle model, we have a fourth-order motor plant. The components of the  $4 \times 4$  matrices  $A$  and  $B$  (Eq. A5) are given in METHODS. The matrix  $A$  has the characteristic polynomial  $\lambda^4 + \alpha_2\lambda^3 + \alpha_1\lambda^2 + \alpha_0\lambda = 0$ , where we used the fact that  $\alpha_0 = 0$ , ascribed to the lack of an elastic term in Eq. 11. Therefore there are one zero eigenvalue and three nonzero eigenvalues ( $\lambda_1, \lambda_2$ , and  $\lambda_3$ ).

Although we could calculate the matrix exponential by explicitly deriving the eigenvalues and eigenvectors, the final expression would be cumbersome without a clear structure. Instead, we evaluate the matrix exponential  $e^{At}$  with the help of the Cayley–Hamilton theorem. According to the theorem, any  $n \times n$  matrix ( $M$ ) satisfies  $p(M) = 0$ , where  $p$  is the characteristic polynomial of  $M$ ,  $p(\lambda) = \det[\lambda\mathbf{I} - M]$ , and  $\mathbf{I}$  is the identity matrix (see, e.g., Strang 2003). By applying the theorem iteratively, any power of  $M$  equal to or higher than its dimensions  $n$  (and any analytical function of  $M$ ) can be reduced to a linear summation of lower powers up to  $n - 1$ , i.e.,  $M^k = \sum_{i=0}^{n-1} c_i M^i$  ( $k \geq n$ ). Therefore for the  $4 \times 4$  matrix  $A$ , the matrix exponential can be expressed as a weighted sum of  $\mathbf{I}$ ,  $A$ ,  $A^2$ , and  $A^3$

$$e^{At} = \phi_0(t) \cdot \mathbf{I} + \phi_1(t) \cdot A + \phi_2(t) \cdot A^2 + \phi_3(t) \cdot A^3 \tag{B1}$$

where  $\phi_i(t)$  ( $i = 0, 1, 2, 3$ ) are functions of time. With this expression, the calculation of matrix exponential is reduced to that of the  $\phi$  function values. To determine the values of  $\phi$ , we diagonalize the above equation

$$e^{At} = \phi_0(t) \cdot \mathbf{I} + \phi_1(t) \cdot \Lambda + \phi_2(t) \cdot \Lambda^2 + \phi_3(t) \cdot \Lambda^3 \tag{B2}$$

where  $\Lambda = \text{diag}(0, \lambda_1, \lambda_2, \lambda_3)$ . By comparing the four diagonal components, we can prove  $\phi_0(t) = 1$ , and derive equations for  $\phi_1, \phi_2$ , and  $\phi_3$

$$\begin{bmatrix} \lambda_1 & \lambda_1^2 & \lambda_1^3 \\ \lambda_2 & \lambda_2^2 & \lambda_2^3 \\ \lambda_3 & \lambda_3^2 & \lambda_3^3 \end{bmatrix} \begin{bmatrix} \phi_1(t) \\ \phi_2(t) \\ \phi_3(t) \end{bmatrix} = \begin{bmatrix} e^{\lambda_1 t} - 1 \\ e^{\lambda_2 t} - 1 \\ e^{\lambda_3 t} - 1 \end{bmatrix} \tag{B3}$$

An explicit solution for  $\phi_1, \phi_2$ , and  $\phi_3$  is not relevant for the following discussion. By evaluating Eq. B1 with  $\phi_0 = 1$  and the  $A$  matrix, we see that the matrix exponential has the following form

$$e^{At_f} = \begin{bmatrix} 1 & \cdot & \cdot & \cdot \\ 0 & \cdot & \cdot & \cdot \\ 0 & \cdot & \cdot & \cdot \\ 0 & \cdot & \cdot & \cdot \end{bmatrix} \tag{B4}$$

The second, third, and fourth columns are complicated functions of  $\phi_1, \phi_2$ , and  $\phi_3$ , which are omitted because they are irrelevant for this proof. With this form of matrix exponential and the initial condition  $x_i = (\theta_i, 0, 0, 0)^T$ , we readily see

$$x_f - e^{At_f} x_i = (\theta_f - \theta_i, 0, 0, 0)^T = (D, 0, 0, 0)^T L_0 \tag{B5}$$

After substituting this expression into the duration Eq. 4, we see that only the (1,1)-component of the  $G^{-1}(t_f)$  matrix survives, and that the duration depends on the movement distance  $D$  only, instead of on  $\theta_i$  and  $\theta_f$  separately

$$\frac{V_f t_f}{K} = \frac{D^2}{L_0^2} (G^{-1})_{1,1}(t_f) \tag{B6}$$

Note that the (1,1)-component of  $G^{-1}(t_f)$  was simply denoted as  $g(t_f)$  in the main text. Because we required the final variance  $V_f$  to be  $(W + w)^2/r^2$ , we obtain the simpler form (Eq. 15). Note that the simpler version of the duration equation holds only when there is no elastic force; the saccade duration derived from the model is dependent on the initial position  $\theta_i$  and final position  $\theta_f$ , instead of on the difference  $\theta_i - \theta_f$  only, because of the elastic term in the eye plant, just as we showed in Fig. 3.

ACKNOWLEDGMENTS

We thank Dr. Daniel M. Wolpert for answering our inquiries on Fitts’s law simulations with the minimum-variance model. We also thank Drs. Vincent Ferrera, Claude Ghez, Pietro Mazzoni, and Terry Sejnowski for helpful discussions and comments.

Present address of H. Tanaka: Computational Neurobiology Laboratory, The Salk Institute for Biological Studies, 10010 N. Torrey Pines Road, La Jolla, CA 92037.

GRANTS

This work was supported by National Eye Institute Grant EY-016270 (formerly MH-054125).

REFERENCES

Abel LA, Dell’Osso LF, Daroff RB, and Parker L. Saccades in extremes of lateral gaze. *Invest Ophthalmol Vis Sci* 18: 324–327, 1979.

Bahill AT, Clark MR, and Stark L. The main sequence, a tool for studying human eye movements. *Math Biosci* 24: 191–204, 1975.

Baloh RW, Sils AW, Kumley WE, and Honrubia V. Quantitative measurement of saccade amplitude, duration, and velocity. *Neurology* 25: 1065–1070, 1975.

Bridgeman B, Hendry D, and Stark L. Failure to detect displacement of visual world during saccadic eye movements. *Vision Res* 15: 719–722, 1975.

Bryson AE and Ho YC. *Applied Optimal Control*. New York: Hemisphere–Wiley, 1975.

Carlton LG. Processing visual feedback information for movement control. *J Exp Psychol Hum Percept Perform* 7: 1019–1030, 1981.

Crossman ERFW and Goodeve PJ. Feedback control of hand movement and Fitts’ law. *Q J Exp Psychol* 35A: 251–278, 1983.

Dornay M, Uno Y, Kawato M, and Suzuki R. Minimum muscle tension change trajectories predicted by using a 17-muscle model of the monkey’s arm. *J Mot Behav* 28: 83–100, 1996.

Eggert T, Mezger F, Robinson F, and Straube A. Orbital position dependency is different for the gain of externally and internally triggered saccades. *Neuroreport* 10: 2665–2670, 1999.

Enderle JD and Wolfe JW. Time-optimal control of saccadic eye movements. *IEEE Trans Biomed Eng* 34: 43–55, 1987.

Feng J, Zhang K, and Wei G. Towards a mathematical foundation of minimum-variance theory. *J Phys A Math Gen* 35: 7287–7304, 2002.

Fitts PM. The information capacity of the human motor system in controlling the amplitude of movement. *J Exp Psychol* 47: 381–391, 1954.

Fitts PM and Peterson JR. Information capacity of discrete motor responses. *J Exp Psychol* 67: 103–112, 1964.

Fitzhugh R. Model of optimal voluntary muscular control. *J Math Biol* 4: 203–236, 1977.

Flash T and Hogan N. The coordination of arm movements: an experimentally confirmed mathematical model. *J Neurosci* 5: 1688–1703, 1985.

Ghez C and Pisa M. Inhibition of afferent transmission in cuneate nucleus during voluntary movement in the cat. *Brain Res* 40: 145–151, 1972.

Hamilton AFC and Wolpert DM. Controlling the statistics of action: obstacle avoidance. *J Neurophysiol* 87: 2434–2440, 2002.

Harris CM. Does saccadic undershoot minimize saccadic flight-time? A Monte-Carlo study. *Vision Res* 35: 691–701, 1995.

Harris CM. On the optimal control of behaviour: a stochastic perspective. *J Neurosci Methods* 83: 73–88, 1998.

Harris CM and Wolpert DM. Signal-dependent noise determines motor planning. *Nature* 394: 780–784, 1998.



- Hogan N.** An organizing principle for a class of voluntary movements. *J Neurosci* 4: 2745–2754, 1984.
- Jones KE, Hamilton AFC, and Wolpert DM.** Sources of signal-dependent noise during isometric force production. *J Neurophysiol* 88: 1533–1544, 2002.
- Keele SW.** Movement control in skilled motor performance. *Psychol Bull* 70: 387–403, 1968.
- Keele SW and Posner MI.** Processing of visual feedback in rapid movements. *J Exp Psychol* 77: 155–158, 1968.
- Nelson WL.** Physical principles for economies of skilled movements. *Biol Cybern* 46: 135–147, 1983.
- Ogata K.** *System Dynamics* (3rd ed.). Upper Saddle River, NJ: Prentice-Hall, 1998.
- Pelisson D and Prablanc C.** Kinematics of centrifugal and centripetal saccadic eye movements in man. *Vision Res* 28: 87–94, 1988.
- Press WH, Flannery BP, Teukolsky SA, and Vetterling WT.** *Numerical Recipes in C*. New York: Cambridge Univ. Press, 1992.
- Robinson DA, Gordon JL, and Gordon SE.** A model of the smooth pursuit eye movement system. *Biol Cybern* 55: 43–57, 1986.
- Schmidt RA and Lee TD.** *Motor Control and Learning: A Behavioral Emphasis*. Champaign, IL: Human Kinetics Publishers, 1998.
- Shadmehr R and Wise SP.** *The Computational Neurobiology of Reaching and Pointing: A Foundation for Motor Learning*. Cambridge, MA: The MIT Press, 2005.
- Smith DR.** *Variation Methods in Optimization*. Englewood Cliffs, NJ: Prentice-Hall, 1974.
- Sober SJ and Sabes PN.** Flexible strategies for sensory integration during motor planning. *Nat Neurosci* 8: 490–497, 2005.
- Stengel RF.** *Stochastic Optimal Control: Theory and Application*. New York: Wiley, 1986.
- Strang G.** *Introduction to Linear Algebra* (3rd ed.). Wellesley, MA: Wellesley–Cambridge Press, 2003.
- Tanaka H, Krakauer JW, Mazzoni P, and Qian N.** Effect of sensory feedback on movement velocity profiles in the extended LQG model of motor planning. Program No. 603.10. *2004 Abstract Viewer and Itinerary Planner*. Washington, DC: Society for Neuroscience, 2004a, Online.
- Tanaka H, Tai M, and Qian N.** Different predictions by the minimum variance and the minimum torque-change models on the skewness of movement velocity profiles. *Neural Comput* 16: 2021–2040, 2004b.
- Todorov E and Jordan JI.** Optimal feedback control as a theory of motor coordination. *Nat Neurosci* 5: 1226–1235, 2002.
- Uno Y, Suzuki R, and Kawato M.** Formation and control of optimal trajectory in human multijoint arm movement. *Biol Cybern* 61: 89–101, 1989.
- van der Geest JN and Frens MA.** Recording eye movements with video-oculography and scleral search coils: a direct comparison of two methods. *J Neurosci Methods* 114: 185–191, 2002.
- van der Helm FCT and Rozendaal LA.** Musculoskeletal systems with intrinsic and proprioceptive feedback. In: *Biomechanics and Neural Control of Posture and Movement*, edited by Winters JM and Crago PE. New York: Springer-Verlag, 2000.
- van Opstal AJ and van Gisbergen JAM.** Scatter in the metrics of saccades and the properties of collicular motor map. *Vision Res* 29: 1183–1196, 1989.
- Williams SR and Chapman CE.** Time course and magnitude of movement-related gating of tactile detection in humans. II. Effects of stimulus intensity. *J Neurophysiol* 84: 863–875, 2000.
- Winters JM and Stark L.** Analysis of fundamental human movement patterns through the use of in-depth antagonistic muscle models. *IEEE Trans Biomed Eng* 32: 826–839, 1985.